



**JOINT INSTITUTE FOR NUCLEAR RESEARCH**  
**Dzhelepov Laboratory of Nuclear Problems**  
**FINAL REPORT ON**  
**THE SUMMER STUDENT PROGRAM**

**$\chi_{c1}$  AND  $\chi_{c2}$  RECONSTRUCTION FROM  $pp$**   
**COLLISION AT  $\sqrt{s_{NN}} = 26\text{GeV}$  at SPD**

Supervisors: Dr. Alexey Guskov

Student: Dario Alberto Ramirez Zaldivar, InSTEC, Havana University, Cuba

Participation period: August 4 - September 28

Dubna, 2019

## Abstract

The study of the contribution of  $\chi_{c1}$  to the total cross-section of  $J/\Psi$  formation could contribute to understanding the polarization puzzle. Estimating of how feasible it is to separate the contributions of  $\chi_{c1}$  from  $\chi_{c2}$  is needed. M spectrum has been reconstructed after smearing the photons and muons momenta coming from  $J/\Psi$  decay simulating the smearing produced in the detection system. The smearing was made using different methods. The Monte Carlo simulation was done at the generator level using Pythia6 and taking into account the transportation of particles inside de detector using SPDRoot. The more significant impact of smearing is carried out by photons. The sigma of the smeared signal is in the same order of the distance between centers of the  $\Delta M_{\chi_{c1/2}}$  peaks. Then it is possible to conclude that the separation of the independent contribution of  $\chi_{c1}$  and  $\chi_{c2}$  can be estimated. Introduction

# Contents

<b>1</b>	<b>Introduction</b>	<b>4</b>
1.1	Studies of Non-Perturbative Quantum Chromodynamics via structure of hadrons and light nuclei . . . . .	4
1.2	Motivation: Using Charmonia production . . . . .	5
<b>2</b>	<b>SPD detector</b>	<b>6</b>
2.1	Magnetic system . . . . .	8
2.1.1	Electromagnetic calorimeter . . . . .	9
2.1.2	Range (muon) system . . . . .	9
2.1.3	Beams . . . . .	10
<b>3</b>	<b>Task</b>	<b>10</b>
<b>4</b>	<b>Results</b>	<b>11</b>
4.1	Generator Level . . . . .	11
4.2	Inside SPD detector: hybrid magnetic field configuration . . . . .	17
<b>5</b>	<b>Conclusion</b>	<b>18</b>
<b>6</b>	<b>Acknowledgment</b>	<b>19</b>

# 1 Introduction

## 1.1 Studies of Non-Perturbative Quantum Chromodynamics via structure of hadrons and light nuclei

Quantum Chromodynamics (QCD) is the only part of Standard Model which exhibits fully non-perturbative (NP) behavior. In this respect, it is similar to the rich and complicated phenomena in condensed matter physics, hydrodynamics, plasma physics, astrophysics, among other subjects. The far-reaching information on NPQCD is provided by its phase diagram and various collective phenomena emerging in heavy-ion collisions, which is studied at BM@N and MPD detectors.

SPD focuses on the complementary way of NPQCD research which is provided by exploring the hadron structure. In modern terms, the latter is described by the vast set of parton distributions and correlations. The most general of them is Wigner function, containing the full information about the longitudinal and transverse spin and partonic momentum degrees of freedom. Averaging over some variables or putting some other to particular (zero) values lead to a more simple and more easily measurable description of fundamental particles. From this reduced description comes the set of Transverse-Momentum-Dependent Parton Distributions (TMDs).

SPD provides a unique opportunity to study various elements of NPQCD hadron structure in the same experiment. It opens the possibility of comparative studies of observable (especially the spin effects) in collisions of hadrons and light nuclei. In this sense, the studies of spin-dependent and spin-independent TMDs is the core of such research.

In general, the exploration of Parton distributions is based on the factorization theorem when the short distance part of the process described by pQCD that uses asymptotic freedom is employed as a kind of microscope to probe the non-perturbative one.

SPD will use several such microscopes. The cleanest process is the production of massive lepton pairs: Drell-Yan (MMT-DY<sup>1</sup>) process. MMT-DY process with one transverse polarized hadron allows one to measure the full set of leading TMDs. It requires to measure the angular distribution of lepton pair in its c.m. frame.

---

<sup>1</sup>Was discovered by Drell and Yan (DY) and, independently, at JINR, by Matveev, Muradyan and Tavkhelidze (MMT).

The production of exclusive MMT-DY pairs provides access to other essential objects -Generalized Parton Distributions, in particular to the ones related to the recently measured pressure of quarks in the proton. Another process sensitive to TMDs (microscope) is J/Psi production. In the case of qq annihilation, there is a duality to MMT-DY process (also known as fusion model) so that J/Psi di-lepton decay plays the same role as MMT-DY itself, with accordingly increased statistics. One more process, sensitive to TMDs is the direct photon production. It provides direct access to various gluon TMDs.

While SPD main target is hadronic collisions, the ultra-peripheral nuclear ones may also be accessible. In the nuclear-proton collisions, such object as Wigner function may be measured. In this scenario, the SPD physical program is mainly faced on the measurement of various npQCD functions, describing the proton structure.

## 1.2 Motivation: Using Charmonia production

The production of  $J/\Psi$  (and charmonia in general) in hadron collisions is of great interest for several reasons. First, the description of the processes is a challenge and an important test for our understanding of QCD.

Although the considerable efforts devoted to the study of charmonia production since the discovery of  $J/\Psi$  and the existence of several theoretical approaches to the problem, a coherent understanding of the process has not yet been obtained. Secondly, a comprehensive understanding of the charmonia production process would allow one to the separation of quark-antiquark annihilation and gluon-gluon fusion contributions. Thirdly, the production process is sensitive to gluon content of colliding hadrons, while experimentally  $J/\Psi$  can be easily reconstructed from the very clean di-lepton modes, making it a powerful tool to probe gluon parton distribution functions (PDF).

It is of particular interest for pion and kaon, since the gluon PDF of the former is poorly known and gluon PDF of the latter has not been measured yet. Inclusive  $J/\Psi$  production is one out of two available experimental methods (along with prompt photons) to probe these gluon distributions in the current and foreseen experiments with pion and kaon beams. It must be noted, that significant fractions (about 40%) of  $J/\Psi$  mesons are produced indirectly through decays of  $\chi_{cJ}$  and  $\Psi(3686)$  (so-called feed-down contributions), thus requiring a dedicated study of these charmonium states. All experimental

applications of the charmonia production rely on our theoretical understanding of the process.

The SPD experiment might be an ideal tool to verify and validate theoretical approaches at relatively low energies and to obtain detailed physical results. The hadronization of the  $c\bar{c}$  can be related to decays of charmonia states or values or derivatives of the heavy quark wave function in the charmonium potential-models. However, these models systematically underpredict the charmonium production rate [1, 2]. Measurements of the difference between the  $\chi_{c1}$ ,  $\chi_{c2}$ , and  $J/\Psi$  polarizations, complementing the observed identity of momentum dependences, represent a decisive probe of NRQCD. Study the contribution of  $\chi_{c1}$  may be a solution to the polarization puzzle [3].

## 2 SPD detector

<sup>2</sup> The design concept of a detector which would be capable to exploit the broad spin physics potential of the high luminosity NICA collider is a one of the main task of the project. The proposed detector design would meet with set of requirements developed on basic the main physics programme tasks given in Chapter 1 and in [21]:

- Close to  $4\pi$  geometrical acceptance;
- High-precision ( $\sim 50\mu m$ ) and fast inner tracker;
- High-precision ( $\sim 100\mu m$ ) and fast tracking system,
- Good particle ID capabilities;
- Efficient muon range system,
- Good electromagnetic calorimeter,
- Low material budget over the track paths,
- Trigger and DAQ system able to cope with event rates at luminosity of  $10^{32} cm^2 s^{-1}$ ,
- Modularity and easy access to the detector elements, that makes possible further reconfiguration and upgrade of the facility.

---

<sup>2</sup>Take from Conceptual design of the Spin Physics Detector [4].

The SPD detector concept matching these requirements is shown in Figure Figure 1 and Figure 2. More detailed description can be found in reference [CDR]. The peculiarity of the SPD general design is the possibility of modernization for a wide range of research in spin physics. For example, upgrade in the barrel part of the SPD without a toroidal magnet will allow to measure prompt photon asymmetries, and study spin effects in reactions with production of different resonances etc. The detailed design of the mechanical supports and platform for the detector are under preparation.

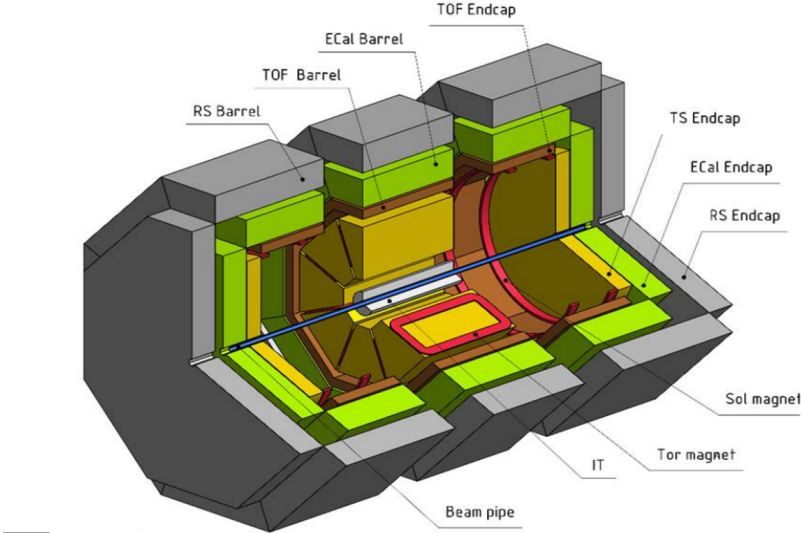


Figure 1: General view of the SPD detector.

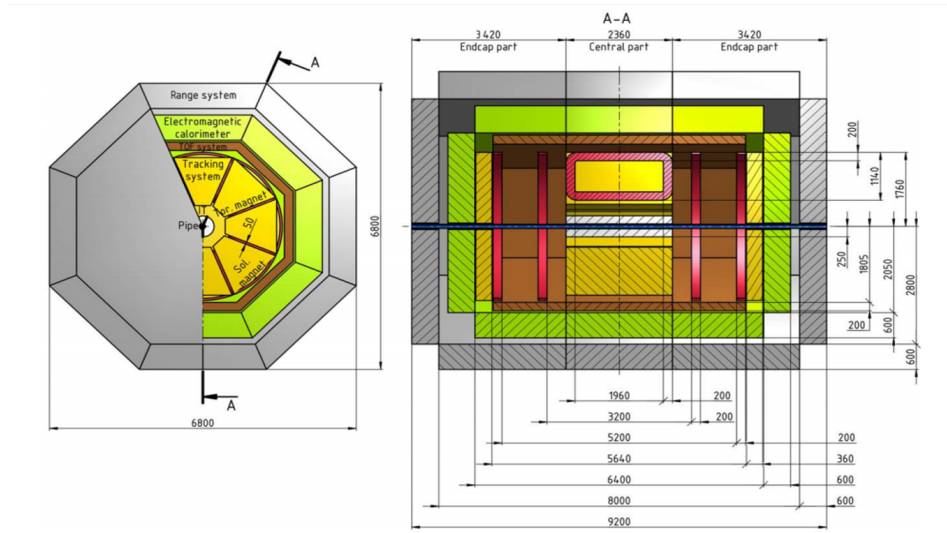


Figure 2: Schematic of the SPD detector with sizes and parts of the detector.

## 2.1 Magnetic system

Basic criteria of the SPD Magnetic System (MS) choice were the following:

- universality, i.e. the field generated elements could be reconfigured to provide optimal distribution of the magnetic field for different physics tasks;
- minimal influence on beam particles spin, i.e. magnetic field of the SPD set-up should be close to zero ( or minimized) along the particle path inside the SPD;
- minimization of the material inside the detector;
- the field integral of (1-2) Tm along the particle track should be provided;
- minimization of the total weight and sizes of the magnetic system (MS) at operating level of the field, i.e. the MS should have proper mechanics.

Several options of the MSs have been considered:

1. solenoid (placed outside ECAL);
2. toroid (inside ECAL): a) coils in barrel part only, b) coils in barrel and in forward and backward parts; c) option b in the case of a room temperature coils; and d) option c in the case of superconducting coils at  $T = 4.2 - 4.5$  K;

3. system of 4 separate coils inside the ECAL: a) all coils are connected in series, and b) pairs of coils connected opposite to each other;
4. combination of the barrel toroid ( 8 coils) and 2 pairs of separate coils. All coils are placed inside the ECal.

The magnetic hybrid configuration used in this report was the fourth. The more important parts for the concerning task are the Electromagnetic Calorimeter and the Range System, because they are where muons and photon will be detected.

### 2.1.1 Electromagnetic calorimeter

The electromagnetic calorimeter (ECAL) of the SPD setup should be placed inside the Range System and will consist of three parts: the barrel part and two end-caps. The ECAL should meet the following requirements coming from the physics tasks [CDR]:

- energy range from 50 MeV to 10 GeV;
- energy resolution of about  $5\%/\sqrt{E[GeV]}$ ;
- granularity 5 cm;
- time resolution 0.5 ns;
- operation in the magnetic field;
- long time stability of the basic parameters 5

### 2.1.2 Range (muon) system

This system serves in the SPD detector for the following purposes:

1. identification of muons in presence of remarkable hadronic background;
2. estimate of hadronic energy (coarse hadron calorimetry).

It is important to stress that the system is the only device in SPD setup, which may identify neutrons. The muon identification (PID) is performed via muonic pattern recognition and further matching of the track segments to the tracks inside the magnets. The precise muon momentum definition is performed by the inner trackers in magnetic field.

### 2.1.3 Beams

Basic specification to available polarization states and combinations is the following:

- protons: vector polarization, longitudinal and transverse direction in respect to a particle velocity;
- deuterons (possibly helium-3 ions at the second stage): vector and tensor polarization, vertical direction of polarization, changing of the polarization direction at  $90^0$  up to about 4 GeV/c momentum;
- possibility to collide any available polarized particles: proton-deuteron, proton-helium-3, deuteronhelium-3 with the luminosity of  $10^{30}cm^{-2}s^{-1}$  at the collision energy equivalent to the proton-proton collisions.
- possibility of asymmetric collisions should be considered as an option for the future development of the facility.
- for efficient estimates of systematic error it is desirable (or necessary) to realize rotation of a bunch polarization direction on  $90^0$  within one turn.

Beam structure of polarized proton and deuteron beams at the first stage will be corresponded to that was optimized for the NICA heavy ion regime. Some of the important, for the SPD, operation parameters in case of bunched beam are the following: bunch number 22, bunch length  $\sigma = 60cm$ , the collider orbit length - 503 m, bunch velocity  $v \approx c = 3 \times 10^8 m/s$ , revolution time  $\tau = 1.6710^{-6}s$ , bunch24 revolution frequency  $f \approx 0.6MHz$ , time gap between bunches  $\Delta\tau = 76.010^{-9}s$ .

As it is clear from the calculations the luminosity level of  $1 \times 10^{30}cm^{-2}s^{-1}$  is reached at a bunch intensity of  $10^{11}$  polarized protons, whereas to obtain the level of  $1 \times 10^{32}cm^{-2}s^{-1}$  multi-bunch storage mode should be used

## 3 Task

Then, to study the feasibility of separation of  $\chi_{c1}$  from  $\chi_{c2}$  the following tasks are proposed:

- Generator level: Using Pythia6 reconstruct  $\Delta M$   $\chi_{c1}$ ,  $\chi_{c2}$  peaks and from minimum bias  $pp$  collision at  $\sqrt{S_{NN}} = 26GeV$ .

Table 1: Mass and radiative decay of  $\chi_{c1}$  and  $\chi_{c2}$ .

Mass <sup>3</sup> (MeV)	$\chi_{c1}(1P)$ $3510.67 \pm 0.05$	$\chi_{c2}(1P)$ $3556.17 \pm 0.07$
The radiative decay <sup>2</sup> : $\gamma J\Psi(1S)$	$(34.31.0)\%$	$(19.0 \pm 0.5)\%$

- Smearing momentum of photons and muons according detection system resolution.

- Check which of muons smearing or photons smearing is more important.

- Check for photon which of energy smearing or direction smearing is more important.

- Inside de SPD detector: Using SPDRoot perform the same analysis using at generator level.

## 4 Results

### 4.1 Generator Level

One way to estimate approximately the contribution of  $\chi_{c1}$  and  $\chi_{c2}$  is to fit the shape of  $\Delta M$  spectrum and determine how many are from each particle. The  $\Delta M$  is the difference between the reconstructed mass of di-muon+photon and the reconstructed mass of di-muon:  $\Delta M = M_{\mu^+\mu^-\gamma} - M_{\mu^+\mu^-}$ . The advantage of following this path is that the uncertainty about the determination of the mass of the muons should be mostly canceled. The work done so far has been done at the generator level using Pythia6. The particles are produced from pp collisions at  $\sqrt{s_{NN}} = 26GeV$ . Figure 3 show the exact mass of reconstructed mass. As expected two sharp peaks are corresponding to  $\chi_{c1/2}$  masses. In Table 1 are shown the exact numerical values. For this purpose the only subprocesses currently switched on are gluon fusion producing  $\chi_{c1/2} + g$ :

Pythia6 command line

`pythia- > SetMSUB(88, 1); //gg- >  $\chi_{c1}g$`

`pythia- > SetMSUB(89, 1); //gg- >  $\chi_{c2}g$`

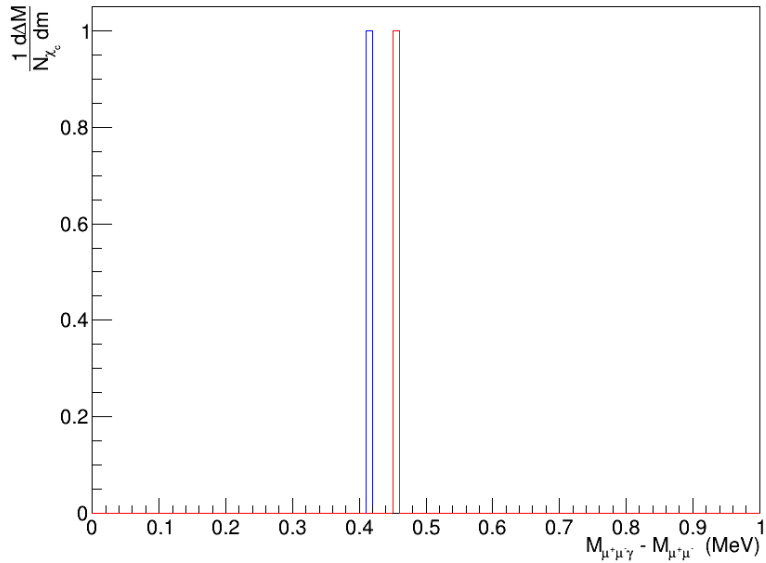


Figure 3: Minimum BIAS mass without smearing, normalized to number of  $\chi_{c1/2}$  : blue plot correspond  $\chi_{c1}$  and red to  $\chi_{c2}$ .

The  $\chi_{c1}$  and  $\chi_{c2}$  are set forced to decay to  $J/\Psi$  and  $\gamma$ . Moreover, the  $J/\Psi$  are set forced to decay to  $\mu^+\mu^-$ . These particles are used to reconstruct the mass spectrum of  $\chi_{c1/2}$ . The 0.7 GeV cut was used for muons momentum because over this energy is impossible to distinguish between muons and pions. For photons, 0.1 GeV cut was employed in the reconstruction process. With photon and the pair of muons from  $J/\Psi$  tetra-momentum vector of  $\chi_{c1/2}$  were reconstructed and consecutively the  $\Delta M$  spectrum. Once the particles were produced the information was saved. The smearing producing by the detection systems was simulated for the muons and photons. For the photons smearing, there are two contributions to take into account. One is geometrical due to detectors dimensions. That was done in this step were two rotation of momentum vector respect to two orthogonal axes. The angle of the rotation was randomly selected under Gaussian distribution with mean value 0 and  $\sigma = 0.01rad$ . Figure 4, 5, and 6 shown the result of switching on/off the smearing in direction and/or magnitude of photons momentum without smearing in muons momentum.

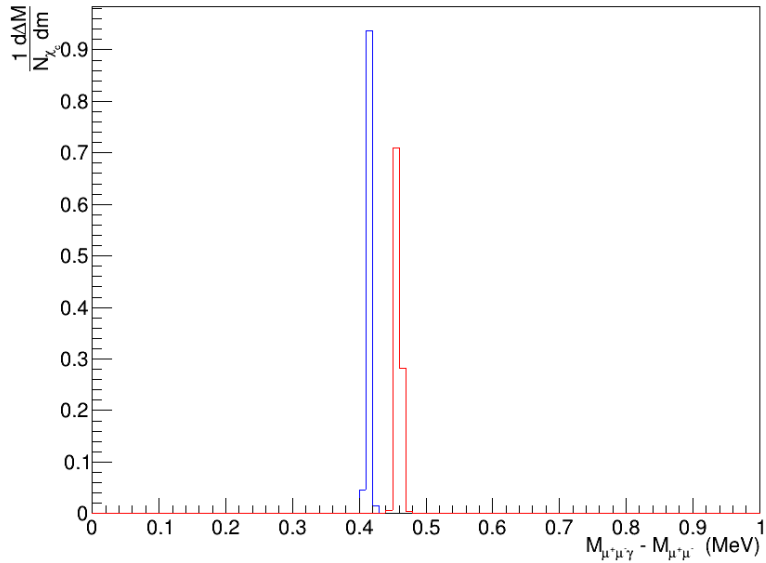


Figure 4:  $\Delta M$  including only Geometrical smearing, normalized to number of  $\chi_{c1/2}$  :  
blue plot correspond  $\chi_{c1}$  and red to  $\chi_{c2}$ .

The second contribution is about energy smearing. This one was done scaling the momentum vector of the photon multiplying it by random number under Gaussian distribution with mean value 1 and sigma equal to  $\frac{5\%}{\sqrt{E}}$ . In the case of muons was used the resolution for theta angle and resolution for the absolute value of momentum to smearing theta angle and momentum respectively. The smearing for muons could be done in two different ways. One was smearing each component of momentum using FWHM as sigma equal to 1% and 2% form  $N(Pi, FWHM)$ . This makes flat smearing because the resolution dependency with angle and momentum is neglected.

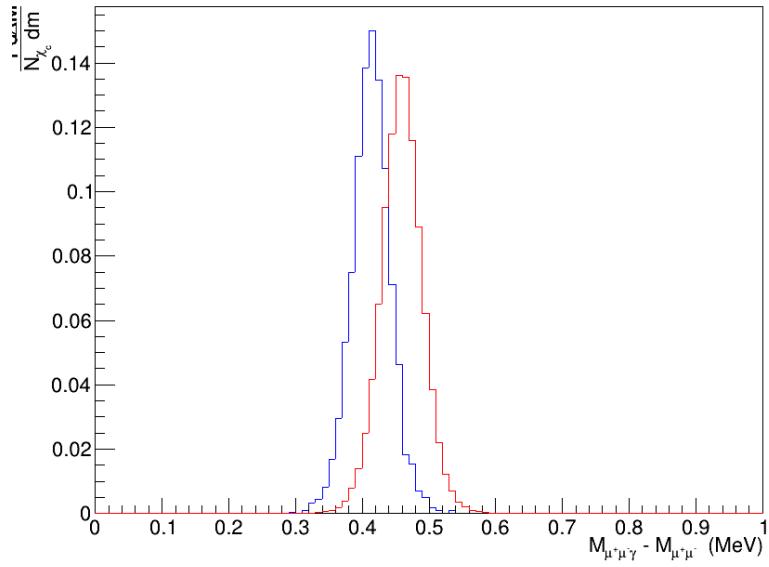


Figure 5:  $\Delta M$  including only Energy smearing, normalized to number of  $\chi_{c1/2}$  : blue plot correspond  $\chi_{c1}$  and red to  $\chi_{c2}$ .

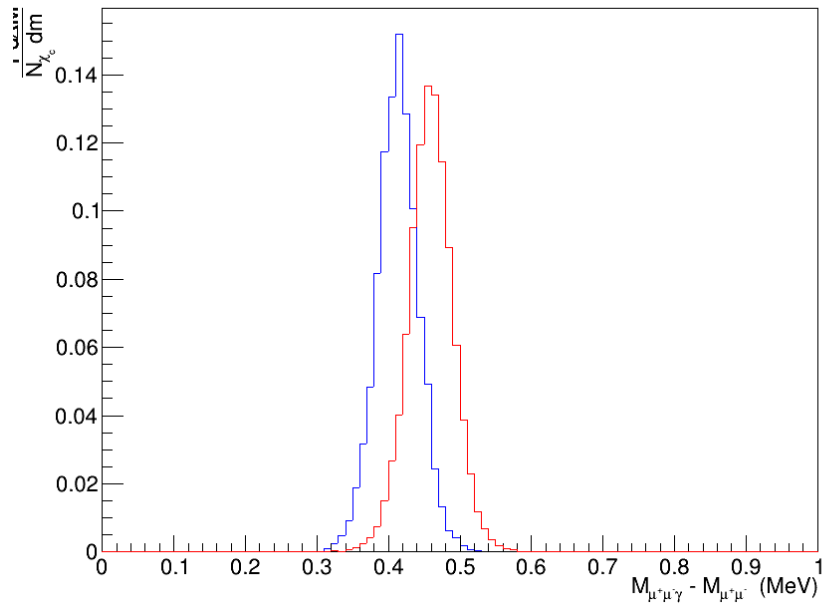


Figure 6:  $\Delta M$  smearing the magnitude and direction of photon momentum, normalized to number of  $\chi_{c1/2}$  : blue plot correspond  $\chi_{c1}$  and red to  $\chi_{c2}$ .

The result of flat smearing for muons are shown in Figure 7. The smearing of 1% and 2% are not so important and even so you can see a difference at the base of the peaks. The other way was selecting the angle and an scaling constant for the absolute value of momentum was done using the following steps.

1. Get theta angle and absolute value of momentum from tetra-vector of muon.
2. Get Momentum Resolution as a function of momentum at 60:  $F(p, 60)$ .
3. Get Momentum Resolution as a function of polar angel at 1 GeV:  $F(1, \theta)$ .
4. Get the ratio  $r_P = F(1, \theta)/F(1, 60)$ .
5. Get the ratio  $r_\Theta = F(p, 60)/F(1, 60)$ .
6. Generate random value for theta  $N(\theta, r_\Theta)$ .
7. Generate random value for momentum  $N(p, r_P)$ .
8. Reconstruct muon tetra-vector.

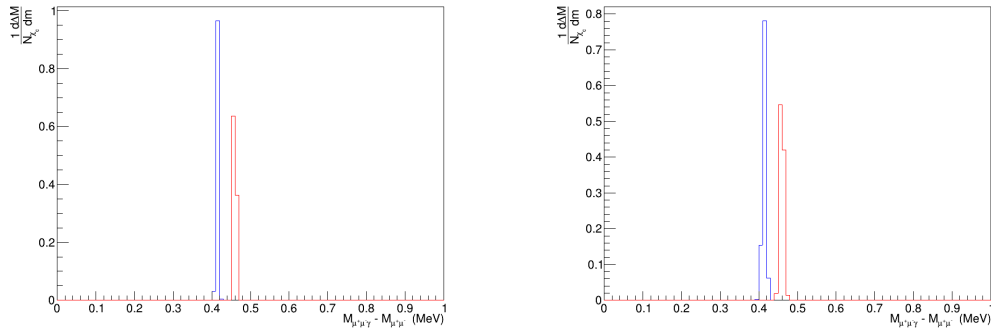


Figure 7: Flat smearing 1% (left) and 2% (right)  $\Delta M$  plot normalized to number of  $\chi_{c1/2}$  : blue plot correspond  $\chi_{c1}$  and red to  $\chi_{c2}$ .

Figure 8 show the smearing produced using a resolution dependence with azimuth angle and momentum magnitude. Flat smearing of 2% and this last one are quite similar and the reason is that the fluctuations in resolution is not too big and the gap between minimum and maximum resolution values is approximately 2% with a central value of around 1.5%. Then is expected that both distributions behave approximately as the same because approximately the same values of resolution are taken.

The global smearing, using resolution dependence with theta and momentum for muons and smearing photon direction and energy is shown in Figure 9. The smearing is dominated for the spread of photons energy with a small contribution of muons.

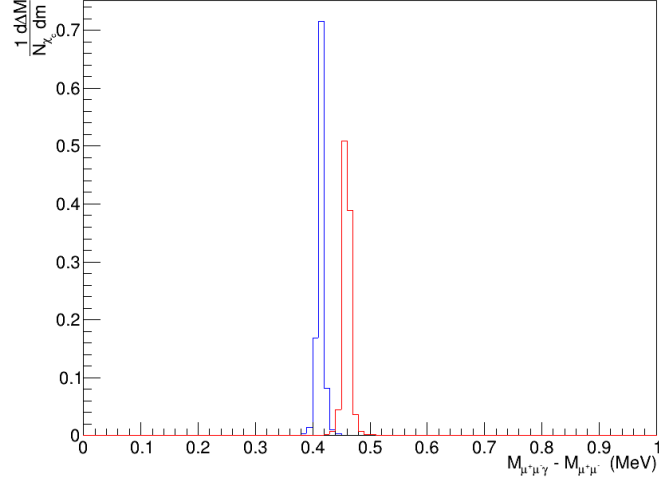


Figure 8:  $\Delta M$  smearing using resolution dependence with momentum and theta angle, normalized to number of  $\chi_{c1/2}$  : blue plot correspond  $\chi_{c1}$  and red to  $\chi_{c2}$ .

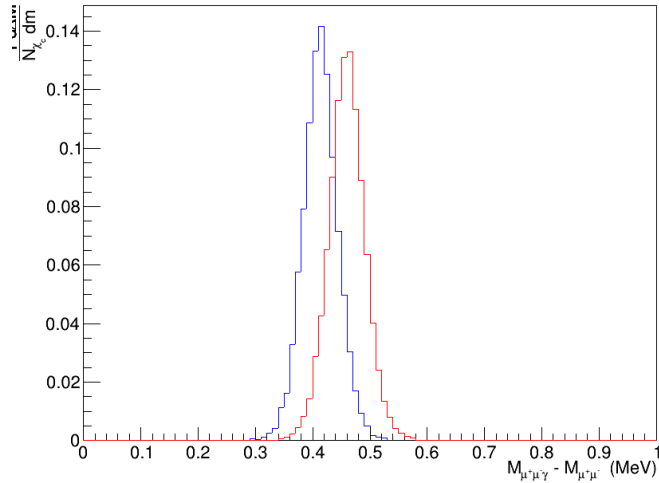


Figure 9:  $\Delta M$  smearing using resolution dependence with momentum and theta angle, normalized to number of  $\chi_{c1/2}$  : blue plot correspond  $\chi_{c1}$  and red to  $\chi_{c2}$ .

## 4.2 Inside SPD detector: hybrid magnetic field configuration

Following a similar idea that was used at generator level, the work was done simulating  $J/\Psi$  production inside the detector coming from the decay of excited states  $\chi_{c1}$  and  $\chi_{c2}$  to  $J/\Psi$  and photon and then smearing angle and momentum magnitude for the final particles. Due to SPDRoot is the software interface used, there is an important difference. Now particles  $\chi_{c1/2}$  are mother particles and then they do not appear on the track and we cannot ask for the daughter and follow the decay chain until we reach muons and photon. Because of this, the reconstruction should be done in the inverse direction: starting from muons and photons and check if they belong to the decay chain of  $\chi_{c1/2}$ . The general outline is described above:

1. Collect all muons that come from  $J/\Psi$ . (cut for momentum  $0.7\text{GeV}$ ). Exclude muons that do not reach Range System (RS).
2. Collect all photons (cut for energy  $0.1\text{ GeV}$ ). Exclude photon that do not reach electromagnetic calorimeter (ECAL).
3. Save the sets of  $J/\Psi$  ( $\mu^+\mu^-$ ) and photons that have the same vertex.
4. Smearing the momentum of  $\mu^+\mu^-$  and photon just already was done at generator level.

These steps are made twice: one is using only  $\chi_{c1}$  subprocess production and the second one using  $\chi_{c2}$  subprocess. For the vertex reconstruction, there is an important point. In principle taking the difference between the photon vertex vector and  $J/\Psi$  vertex vector as zero has no problem. But to have simulation result near to real method of vertex reconstruction should be taking into account the error of the method. Then is possible to include a pair of  $J\Psi$  and photon produced at a distance different from zero. To make Monte Carlo correction you should know how big is the difference between the results with and without using vertex reconstruction method error. At the moment, the distance between vertex will have no error and it will be taken as zero.

Another important fact is that the magnitude for tetra-momentum vector of particles is taken as the momentum at the entrance of ECAL in case of photons. Due to the reconstruction of muons momentum is very precise [5] the momentum is set as at the vertex and there are no need to take the momentum at entrance of Range System.

Once these steps are done the  $\Delta M$  spectrum is plotted (Figure 10). Is remarkable the main difference between the Monte Carlo at generator level and inside SPD detector is

that the bases of the  $\chi_{c1/2}$  are wider. There are two main reasons for this: one because multiple scattering with detectors material makes and additional smearing to the energy of particles if the momentum is taken at the entrance of detection material; and second one is because some reconstruction of  $\chi_C$  are made using set of  $\mu^+\mu^-\gamma$  where one photon could not come from the decay in question. For the last reason, photons with too high momentum are excluded.

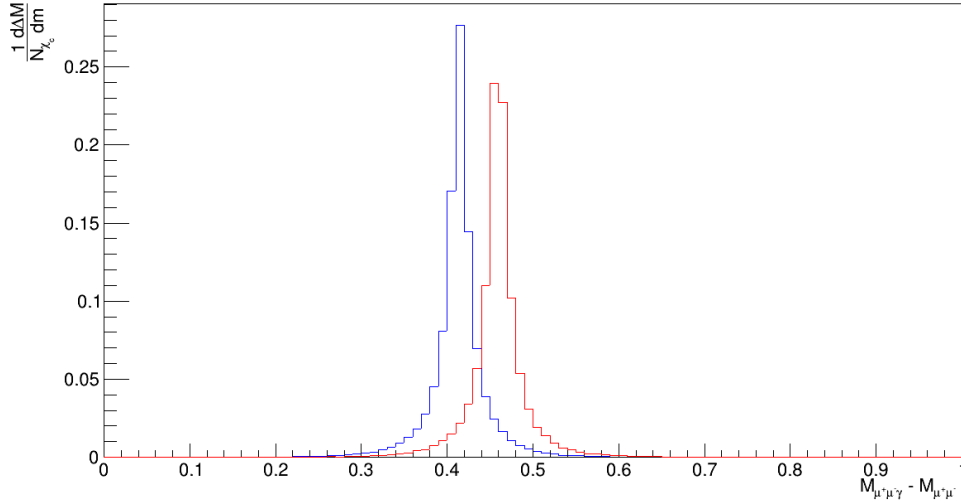


Figure 10:  $\Delta M$  plot normalized to number of  $\chi_{c1/2}$  : blue plot correspond  $\chi_{c1}$  and red to  $\chi_{c2}$ .

## 5 Conclusion

After study the  $\Delta M$  distribution at generator level and inside SPD detector geometry, smearing muons and photons momentum using different methods, we can conclude :

- The higher contribution to the signal spread is the energy resolution of photon with a small contribution from about 2%.
- Separation of  $\chi_{c1}$  and  $\chi_{c2}$  peak is feasible due to the separation between them is about  $1\sigma$  obtained using Monte Carlo.
- Improvement can be done to this work using better data for muons resolution dependence with angle and momentum.

## 6 Acknowledgment

To Alexey Guskov for his guidance throughout my stay even when he was not physically present.

To Igor Denisenko for his absolute support in the difficult parts of the job and his great patience to explain my doubts over and over again.

To Fernando Guzman, from InSTEC (UH), Cuba, for his unconditional help, his wisdom and friendship.

To Antonio and Ileana for making my stay in Dubna nice to make me feel at home. To my eternal friend Jorge Luis for supporting me with the necessary debates to overcome circumstantial obstacles of the project.

To the rest of the colleagues who supported me in the technical part with the Computer Center.

## References

- [1] T.H. Chang, M.E. Beddo, C.N. Brown, T.A. Carey, W.E. Cooper, C.A. Gagliardi, G.T. Garvey, D.F. Geesaman, E.A. Hawker, X.C. He, L.D. Isenhower, D.M. Kaplan, S.B. Kaufman, D.D. Koetke, G.S. Kyle, P.L. McGaughey, W.M. Lee, M.J. Leitch, J.M. Moss, B.A. Mueller, V. Papavassiliou, J.C. Peng, G. Petitt, P.E. Reimer, M.E. Sadler, W.E. Sondheim, P.W. Stankus, R.S. Towell, R.E. Tribble, M.A. Vasiliev, J.C. Webb, J.L. Willis, and G.R. Young.  $J/\psi$  polarization in 800-gev pcu interactions. *Phys.Rev.Lett.*91:211801, 2003.
- [2] M. Beneke and I.Z. Rothstein. Hadro-production of quarkonia in fixed target experiments. *Int.J.Mod.Phys.A*12:3857-3866, 1997.
- [3] Pietro Faccioli, Carlos Loureno, Mariana Arajo, Joo Seixas, Ilse Krtschmer, and Valentin Knnz. From identical s- and p-wave pt spectra to maximally distinct polarizations: probing nrqcd with  $\chi$  states. *Eur. Phys. J. C*, 2018.
- [4] JOINT INSTITUTE FOR NUCLEAR RESEARCH. Conceptual design of the spin physics detector, October 27, 2018.
- [5] Igor Denisenko. Talk: Physics with charmonia at spd. dspin, 2019.